Journal of Structural Geology, Vol. 13, No. 10, pp. 1111 to 1124, 1991
Printed in Great Britain

0191-8141/91 $03.00+0.00

A model for the development of a domainal quartz *c*-axis fabric in a coarse-grained gneiss

FRANK FUETEN

Department of Geological Sciences, Brock University, St. Catharines, Ontario, Canada L2S 3A1

PIERRE-YVES F. ROBIN and RON STEPHENS

Center for Tectonophysics, University of Toronto, Mississauga, Ontario, Canada L5L 1C6

(*Received* 22 *May* 1990; *accepted in revised form* 27 *April* 1991)

Abstract—Quartz *c*-axis fabrics in high-grade coarse-grained layered gneisses reveal a distinctive pattern, with three perpendicular maxima, which can be interpreted in terms of syntectonic recrystallization and growth. Mapping of the distribution of *c*-axes within a single thin section demonstrates that the fabric is domainal. Fabric domains are on the scale of millimetres and are associated with individual quartz-rich patches. No single domain exhibits the overall fabric of the complete thin section. Within each domain, weighting of the *c*-axis fabric by the area of each quartz grain demonstrates that the largest grains have their *c*-axes preferentially at the maxima.

A model is presented to account for the development of this fabric. Grains which can keep their stored strain energy to a minimum by the use of a single glide system, oriented approximately parallel to the plane and direction of maximum resolved shear stress, grow at the expense of other grains. The largest, most successful grains deform by glide on only one of either the basal ⟨*a*⟩ or the prism ⟨*a*⟩ systems, depending on the crystallographic orientation of the grain. Each domain develops its own glide direction by co-operation of the glide systems of its constituent grains. The successful grains in a domain are those which can accommodate that direction. The bulk strain of the rock is achieved by the addition of the strains distinct to each domain.

INTRODUCTION

QUARTZ *c*-axis fabrics are a powerful tool for the interpretation of the deformation of quartz-rich rocks. Classical models for the development of such fabrics have been based on the rotation of grains as a result of glide (Etchecopar 1977, Lister *et al.* 1978); these models predict girdle concentrations on spherical nets. Recent workers (e.g. Burg *et al.* 1986, Urai *et al.* 1986, Jessell 1988) have recognized the importance of recrystallization in fabric development. A number of workers (e.g. Eisbacher 1970, Sander 1970, Garcia Celma 1982, Knipe & Law 1987, Law *et al.* 1990) have also observed that fabrics are often domainal rather than homogeneous on the scale of a thin section.

The purpose of this paper is to present a model of fabric development in high-grade gneisses. The model is based on a detailed analysis of two specimens of gneisses from the Proterozoic-aged Thompson Belt, Canada. These gneisses are composed of alternating quartz-rich and quartz-poor layers and have *c*-axis fabrics that commonly show two or three mutually perpendicular maxima. The model specifically incorporates recrystallization and accounts for the domainal nature of the fabric as well as for the occurrence of point maxima rather than girdles.

Similar patterns have been reported from Saxony granulites by a number of workers (Sander 1970, Hoffman 1972, 1975, Starkey 1979, Behr 1980, Lister & Dornsiepen 1982). The positions of the maxima are numbered I and III (Fig. 1). This terminology, which follows that of Lister & Dornsiepen (1982), is modified after Behr (1961) and originates from Fairbairn (1949) and Sander (1970). Maximum I lies at the *Y* position, i.e. in the plane of foliation and perpendicular to the lineation. The two Maxima III lie in the *XZ* plane, which contains the lineation but is perpendicular to the plane of foliation; they are positioned 45° away from the lineation and therefore bisect the *X* and *Z* axes. In an equal-area projection parallel to *XZ* (Fig. 1), each Maximum III appears as a concentration on diametrically opposed sides of the net, and Maximum I lies in the centre of the net.

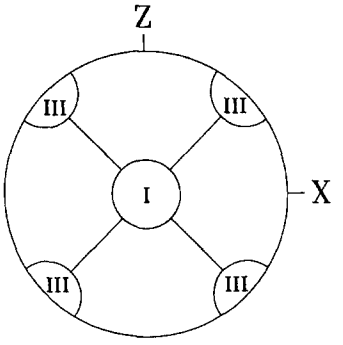

Fig. 1. Position of kinematic axes (*X* = lineation, *Z* = normal to foliation) and *c*-axis fabric maxima.

In the Saxony granulites, the origin of *c*-axis fabrics dominated by these maxima has been explained in several ways. Hoffman (1972) interprets such patterns by the 'fracture hypothesis' and notes a relationship between the development and sharpness of Maximum I and the presence of micas. Starkey (1979) attributes Maximum I to slip on the prism ⟨*a*⟩ system. He suggests

that Maxima III are due to slip on positive and/or negative rhombs (r, z), but also finds evidence (Starkey 1979, fig. 11) that basal slip may have been important in some cases. Lister & Dornsiepen (1982) interpret this fabric as a Type II crossed girdle (Lister & Williams 1980), and suggest it might be achieved by a balance between slip on the basal $\langle a \rangle$ and prism $\langle c \rangle$ systems because it mimics some details of fabrics obtained by the Taylor–Bishop–Hill model. Metamorphic conditions, variations in the deformation path, and strain-rate are thought to influence the choice of glide systems. Based on symmetry arguments (Sander 1970, Hoffman 1972), experimental evidence (Green *et al.* 1970), and evidence resulting from numerical modelling (Lister & Hobbs 1980, Lister & Dornsiepen 1982), this fabric has been interpreted as a flattening fabric.

GEOLOGICAL SETTING

The Thompson Belt (Fig. 2), located in northern Manitoba, is a linear, NE-trending deformation belt at the border of the Churchill Province and the Pikwitonei region of the Superior Province, Canadian Shield. It is thought to result from plate collision during the Hudsonian orogeny, dated in the Thompson Belt as between 1.9 and 1.6 Ga (e.g. Green *et al.* 1985). Rocks within the Thompson Belt consist mainly of a series of felsic gneisses that are considered to be the retrogressed equivalents of the Kenoran Pikwitonei granulites (Scoates *et al.* 1977, Weber & Scoates 1978). Recent work (Fueten & Robin 1989) shows that the belt was the site of predominantly dip-slip movement with a Superior-side over Churchill-side sense for the recognizable part of its ductile deformation history.

In the central portion of the Belt, on Paint Lake (Fig. 2), a granulite-grade metamorphism is preserved (Fueten & Robin 1989). Paktunç & Baer (1986) estimate recorded temperatures ranging from 700 to 850°C and pressures of 0.9–0.97 GPa. The granulite-grade mineral assemblages are altered in parts of the area, the degree of alteration ranging from minor to almost complete replacement of orthopyroxene. It is within the central portion of Paint Lake that fabric analysis of eight samples showed patterns dominated by Maxima I and III (Fueten 1989). The samples come from a shear zone, several kilometres in thickness, with a vertical foliation and down-dip stretching lineation. Kinematic indicators show that the southeast side moved up with respect to the northwest side (Fueten & Robin 1989).

Table 1. Modal analyses of samples (visual estimates)

	Sample 85-16 (%)	Sample 86-251 (%)
Quartz	35	20
K-feldspar	40	35
Plagioclase	1	5
Hornblende	15	0
Biotite	5	30
Clinopyroxene	2	0
Sericite	0	5
Chlorite	5	5

The mineralogy of the Paint Lake samples analysed here does not record the granulite-grade metamorphism (see Table 1), but other samples (Fueten 1989, samples 6-199 and 6-560) exhibiting similar c-axis patterns still contain undeformed orthopyroxene. The fabrics studied here could thus have formed under metamorphic conditions ranging from granulite to amphibolite grade. By comparison, the Saxony granulites record granulite grade metamorphic conditions of approximately 700–900°C and 0.4–0.65 GPa (Behr 1980), but developed c-axis patterns similar to the ones found here under

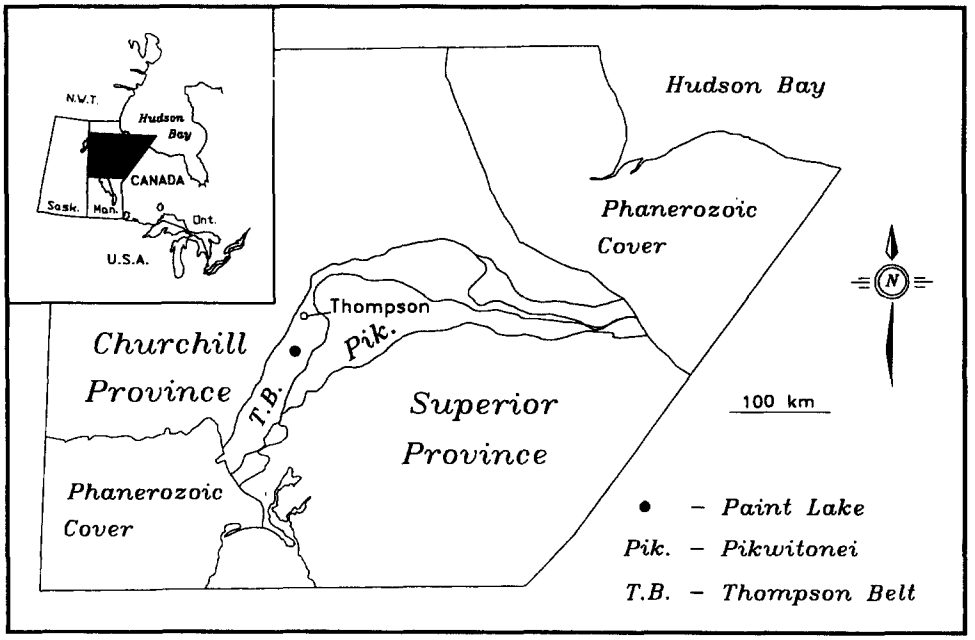

Fig. 2. Location of Thompson Belt and Paint Lake, Manitoba, Canada.

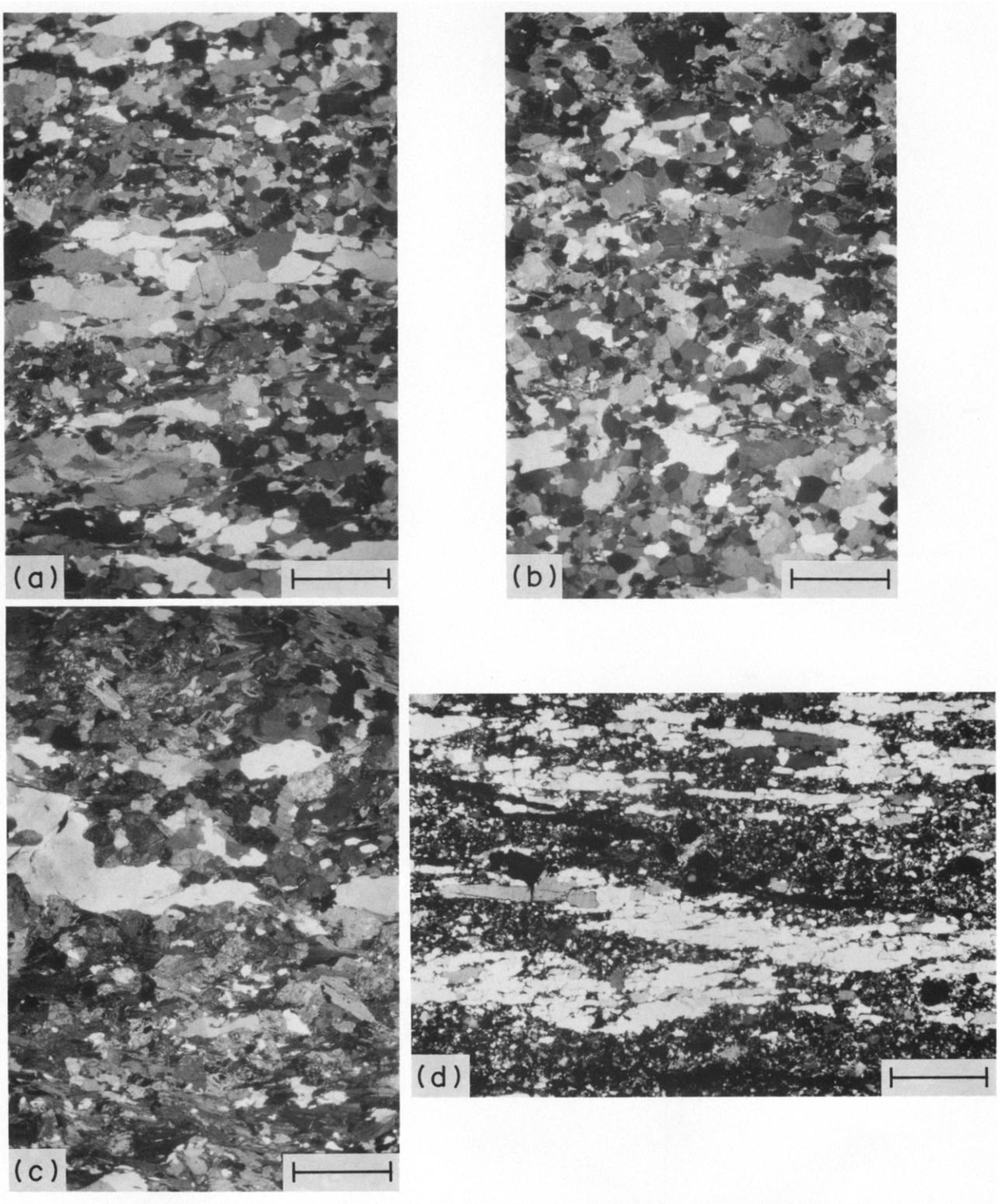

Fig. 3. Photomicrograph of (a) section 85-16, (b) section 85-16A, (c) section 86-251. (d) Saxony granulite specimen 68/126A used by Starkey (1979) and provided by Dr J. Starkey. (a), (c) and (d) are cut parallel to XZ, (b) is cut perpendicular to the lineation (parallel to ZY). Note differences in grain-sizes and grain shapes between (a–c) the Thompson Belt sections and (d) the Saxony granulite section. Scale bars = 1 mm.

amphibolite facies metamorphic conditions (Starkey 1979). Figures 3(a)–(c) contrast the three sections examined in this study with the Saxony granulite specimen 68/126A (Fig. 3d) used by Starkey (1979).

None of the *c*-axis patterns shows all maxima (I, III) (Fueten 1989). Each is a subset of the complete pattern, Maximum I being most commonly absent. However, no single Maximum III is present without at least a less developed Maximum III in the adjacent quadrant of the spherical projection. Similarly, individual samples from the Saxony granulites do not contain all maxima, and the composite diagrams presented by Lister & Dornsiepen (1982, figs. 4c–h) contain the maxima of several individual fabric diagrams.

In some rocks, a segregation into quartz-rich and quartz-poor layers is present. Quartz within these sections occurs both as disseminated grains and as aggregates of closely spaced quartz grains. The grain boundaries between adjoining quartz grains are smooth. The aggregates are generally longer parallel to the foliation than they are wide across the foliation. It is within these aggregates that the largest grains occur.

TECHNIQUE

Two hand-samples were selected: one shows a very well developed segregation; the second contains quartz distributed more homogeneously throughout the rock. Two thin sections were cut from the first sample, one (85-16) containing the *XZ* plane, the second (85-16A) containing the *YZ* plane. Sections 85-16 and 85-16A were chosen so that the same quartz-rich and mafic-rich layers were present in both thin sections. One thin section (86-251) was cut from the second sample containing the *XZ* plane.

Colour photographs were taken under crossed polars and a photo-mosaic with a final magnification of 19.6:1 was produced. Individual quartz grains and subgrains were mapped on a sheet of acetate taped to the top of the photo-mosaic. The distinction between grains and subgrains was made on the basis of the sharpness of the boundary. Quartz grain boundaries were sharp. This corresponded to a lattice rotation of more than 10° between neighbouring grains. In contrast, subgrains had lattice rotations across their boundaries between 2° and 10°.

TIMING OF GRAIN GROWTH RELATIVE TO DEFORMATION

In the samples examined, the grains are large and grain boundaries are straight. This could be the result of annealing after the deformation ceased as the temperature remained high; during a period of static recrystallization grain boundaries may straighten out, and some low internal strain energy grains may increase in size by grain boundary migration. Culshaw & Fyson (1984) argue that their *c*-axis fabric was indeed modified during a period of metadynamic recrystallization (McQueen & Jonas 1975), when dynamically nucleated grains continued to grow statically immediately after cessation of the deformation. The crystallographic fabric of such a rock would thus not be a direct record of the deformation. It is therefore important here to attempt to demonstrate that the fabrics in our coarse-grained gneisses were acquired during deformation. Grain-size and subgrain-size paleopiezometry (Mercier *et al.* 1977, Twiss 1977, 1986, Weathers *et al.* 1979, Christie & Ord 1980, Kohlstedt & Weathers 1980, Ord & Christie 1984) can potentially be used to decide if both grains and subgrains are in size equilibrium with each other. If the differential stresses interpreted from both grain-size and subgrain-size are in agreement with each other, then both grains and subgrains can be argued to be the result of the same deformational event.

Grain-sizes were measured under the microscope. Figure 4 shows the range of differential stresses estimated from grain- and subgrain-sizes for a variety of calibrations. There are obvious limitations to the use of paleopiezometry in coarse-grained gneisses, for example: grains and subgrains are much larger than those used for calibration of paleopiezometry; the gneisses are polymineralic whereas the models, and the calibration, are for monomineralic rocks; new grains may form by subgrain rotation as well as by recrystallization. Despite the uncertainties, there is considerable overlap between the ranges of differential stresses obtained for both paleopiezometers. We therefore suggest that the evidence is compatible with the formation of grains and subgrains in the same event. Note however that the upper limit of stress inferred from the grain-sizes is higher than that inferred from the subgrains. A simple explanation may be that equilibration of the subgrains took place at reduced stresses, during the waning stages of the deformation that had produced the grains.

CRYSTALLOGRAPHIC ORIENTATIONS

Use of weighting c-axis orientation data

c-axis orientations of quartz grains and individual subgrains were measured using a four-axis universal stage (e.g. Turner & Weiss 1963, pp. 197–203). Counting and contouring used a continuous spherical Gaussian counting function as described by Robin & Jowett (1986). Data were counted in two ways: (1) unweighted method, each orientation datum was assigned the same weight; (2) weighted method, each *c*-axis measurement was weighted proportionately to the area of the corresponding grain. Thus a grain with dimensions of 1 cm^2 has the same weight as 100 grains measuring only 1 mm^2. A standard result of stereology, used in modal analysis of rocks (e.g. Chayes 1956), is that areal ratios of three-dimensional objects as seen in a two-dimensional section are an estimate of the volumetric ratios of these objects in three dimensions. The weighting makes the data comparable to an X-ray analysis in which the strength of

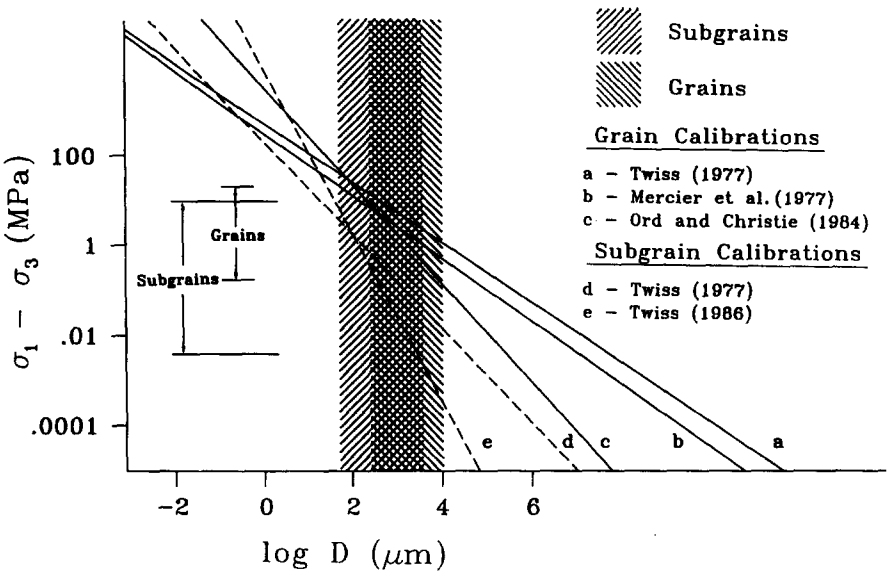

Fig. 4. Differential stress inferred from grain- and subgrain-size. Ranges of grain-size and subgrain-sizes present are indicated by hachures. The range of differential stresses inferred is calculated for grains from all of the a, b, and c calibrations, and for subgrains from Twiss's (1986, fig. 12, curve 1) calibration based on experimental data.

a signal is directly proportional to the area from which it is diffracted.

Weighting measurements by their grain areas can have a dramatic effect on the shape of the contours and, therefore, has important implications when large grain-size variations are present, as in the samples investigated here. For example, section 85-16 (Fig. 5a) contains few large grains with steeply plunging *c*-axes, which have no significant representation when the unweighted data is contoured, but are responsible for the central maximum and for the peak value (mode) when the weighting procedure is applied. Section 86–251 (Fig. 6) illustrates the effect that a single large grain (25% of total quartz) can have on the weighted data. Figure 6(c) shows contours of the weighted data with the largest grain removed. The shape of the contours do not change very much, but the peak value in Fig. 6(c) decreases to less than half of that in Fig. 6(b). This indicates that Maximum III is not due solely to one grain, but that one grain can be responsible for greatly changing the height of that peak.

Whole section data

In section 85-16 (parallel to *XZ*, Fig. 5a), contouring of the weighted data enhances the NE maximum and a strong peak at Maximum I appears, while some of the shallow plunging clusters present in the unweighted data disappear. In section 85-16A (parallel to *YZ*, Fig. 5b), the data have been rotated into the same orientations as Fig. 5(a). Since section 85-16A has fewer large grains than section 85-16, weighting of the data has a less dramatic effect. The fabrics probably differ because they sample different grain populations. We suggest, however, that there are important similarities. In both sections, Maximum I and the NE Maximum III are enhanced by the weighting technique, whereas the NW Maximum III decreases.

In section 86-251 (parallel to *XZ*, Fig. 6), the contoured unweighted plot (Fig. 6a) has the highest symmetry of all three sections with the two Maxima III being almost equally well developed. Weighting of the data (Fig. 6b) dramatically changes the symmetry of the patterns. A peak located between 15° and 20° away from *Y* (Maximum I) appears and one Maximum III becomes dominant.

Domainal distribution

To map the distribution of *c*-axis orientations across a section (A.V.A., Sander 1970), a small arrow, representing the *c*-axis trend, with the plunge numerically written beside it, was drawn over each grain on the thin section map. This plot provided the basis for observing *c*-axis patterns over the scale of the thin section. Each section was then subdivided into domains on the basis of *c*-axis pattern characteristics and grain distribution (Figs. 7–9). Where possible, the layers provided a convenient definition of the boundaries used to divide one domain from another. We attempted to keep the size of the individual domains as large as possible.

Section 85-16 was subdivided into six domains (Fig. 7). The contoured weighted fabrics indicate that each domain tends to show one dominant orientation of *c*-axes with peaks that alternate from domain to domain. For example, domains 2 and 4 (Fig. 7) show peaks in the NE quadrant, whereas domain 3 exhibits a peak in the NW quadrant. Domains 1, 5 and 6 have peaks at Maximum I with minor extensions along the crossed girdle. The fabric for the whole section (upper right of Fig. 7), is not exhibited by any one domain.

The mineral layering in section 85-16A corresponds to

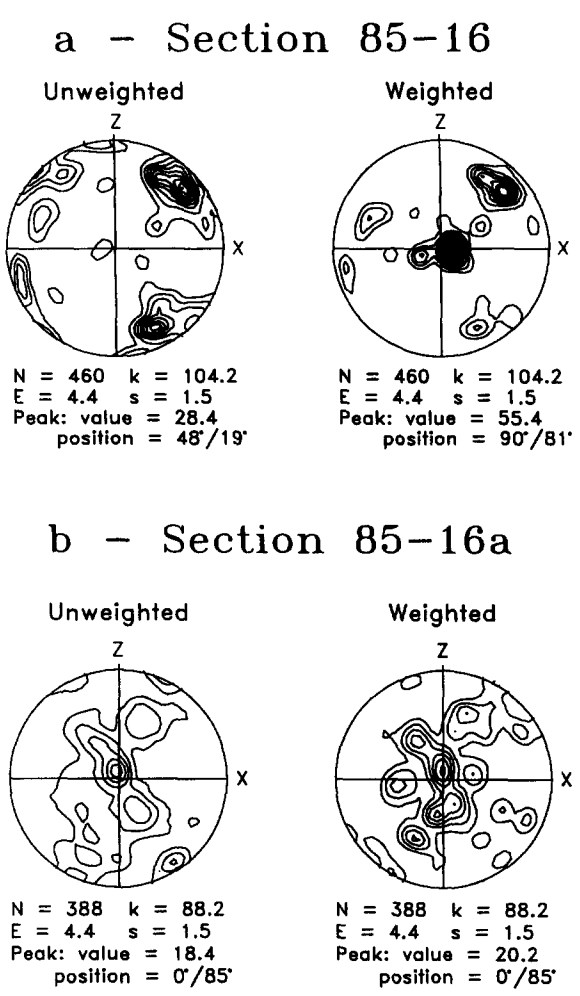

Fig. 5. Quartz *c*-axis orientation data, counted using the method described by Robin & Jowett (1986). (a) Section 85-16, unweighted and weighted data. (b) Section 85-16A, unweighted and weighted data. Rather than a counting circle, the method uses a continuous spherical gaussian counting function. The kurtosis (k), of the gaussian function is calculated from the number of data points (N), using $k = 1 + N/9$. This value of k leads to $E = 3\sigma$, where E is the expected value of counts for N data points evenly distributed over the hemisphere, and σ is the expected standard deviation of counts if N data points are drawn randomly from an isotropic population (Robin & Jowett 1986). The lowest contour shown corresponds to counts equal to E. Higher contours are every 2σ.

that in section 85-16 and domains were selected to correspond also. The peaks in section 85-16A (Fig. 8) are lower than in section 85-16 and do not alternate as well from domain to domain. This correlates with the lack of large dominant grains in section 85-16A. It may also indicate that the fabric varies more rapidly perpendicular to the lineation than parallel to it, and that the domains as we have chosen them may be too large. Domains 1, 2 and 6 (Fig. 8) have peaks at Maximum I. In domains 2 and 4 the extensions of the peaks are along the same two quadrants as in the corresponding domains in section 85-16. As in section 85-16, no domain mimics the fabric of the whole section.

In section 86-251 (Fig. 9), domain 5 is dominated by a few large grains and shows a strong Maximum III and an accessory Maximum I. Domains 1 and 2 exhibit Maxima III in both quadrants. Domains 3 and 4 do not show clear patterns. Because domain 4 consists mostly of widely isolated quartz grains, an attempt was made to find distinctive patterns by subdividing it into four subdomains. Of these, subdomain 4b, shows two distinct maxima in two adjacent quadrants of the net. However, no single domain or subdomain mimics the fabric of the complete section.

In conclusion, the *c*-axis patterns produced by the individual domains never show the pattern exhibited by the complete section, and the *c*-axis pattern for the complete section is only obtained by the combination of the peaks from all the subdomains. Consequently, the symmetry of the overall pattern is higher than that of any one domain. Section 85-16 has well-developed alternating domainal patterns, and two adjacent domains are sufficient to approximate the overall pattern of the section. The domainal patterns are best developed (i.e. they contain the highest peaks and the smallest number of minor peaks), when the quartz grains involved are large and concentrated in quartz-rich layers, as in section 85-16 and domain 5 of section 86-251. Grain-size and grain proximity must therefore be important factors in the development of the fabric.

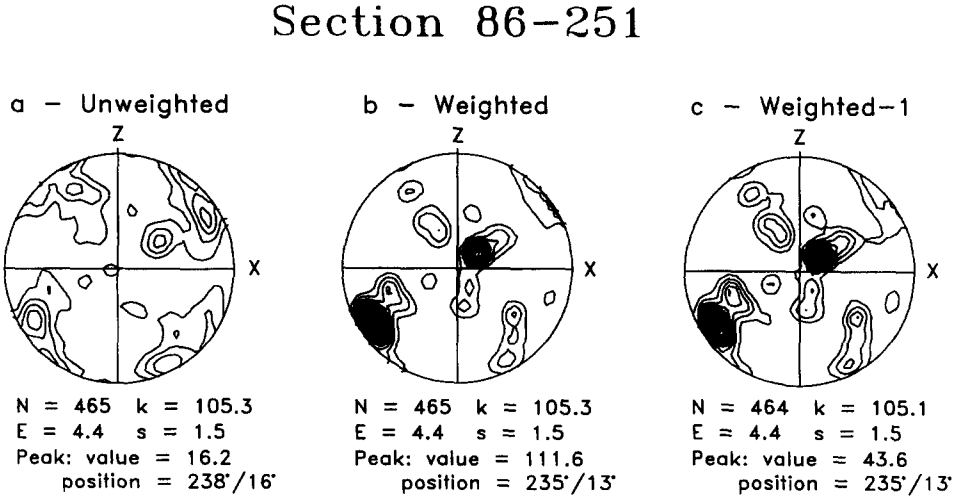

Fig. 6. Quartz *c*-axis orientation data from section 86-251. (a) Unweighted data. (b) Weighted data. (c) Weighted data without the largest grain which accounts for 25% of total quartz in the section.

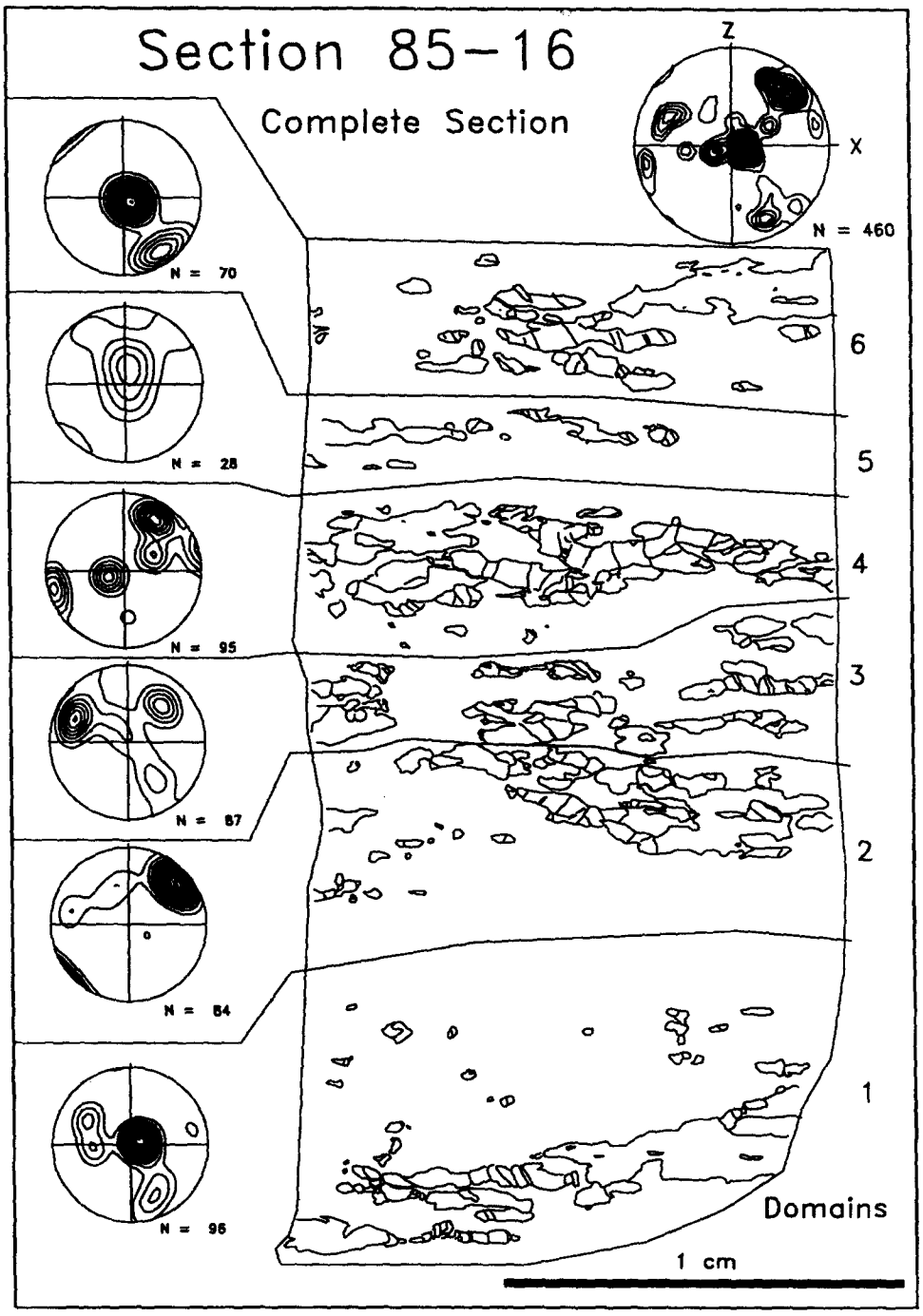

Fig. 7. Domains and domainal fabrics for section 85-16.

DISCUSSION

Grain-size and crystallographic orientation

Large quartz grains in deformed rocks may result from several different processes. Bouchez (1977) demonstrated that the quartz ribbons in a Hercynian shear zone, deformed under sub-greenschist facies metamorphism, formed by the deformation of large porphyroclasts. The quartz ribbons studied by Bouchez (1977) are shaped like stretched ellipses, the long sides of which lie within one foliation plane and are quite planar. Here, there is no evidence that the gneisses had large grains that may have served as precursors for the large quartz grains. The cross-sectional area of the large quartz grains may be more than one order of magnitude greater than the areas of any other mineral grains in the rock. The large grains examined here have irregular shapes that span several foliation planes (e.g. section 85-16, domain 6). Their shape and size suggest that the large grains originated by incorporating several smaller grains into large ones. Such coalescence of several grains into ribbon grains has been observed by Means & Dong (1982) and Urai *et al.* (1986) during the deformation of para-dichlorobenzene, and has been modelled by Jessel (1988).

Large grains could also form during a period of static annealing, but we have argued above that the correspon-

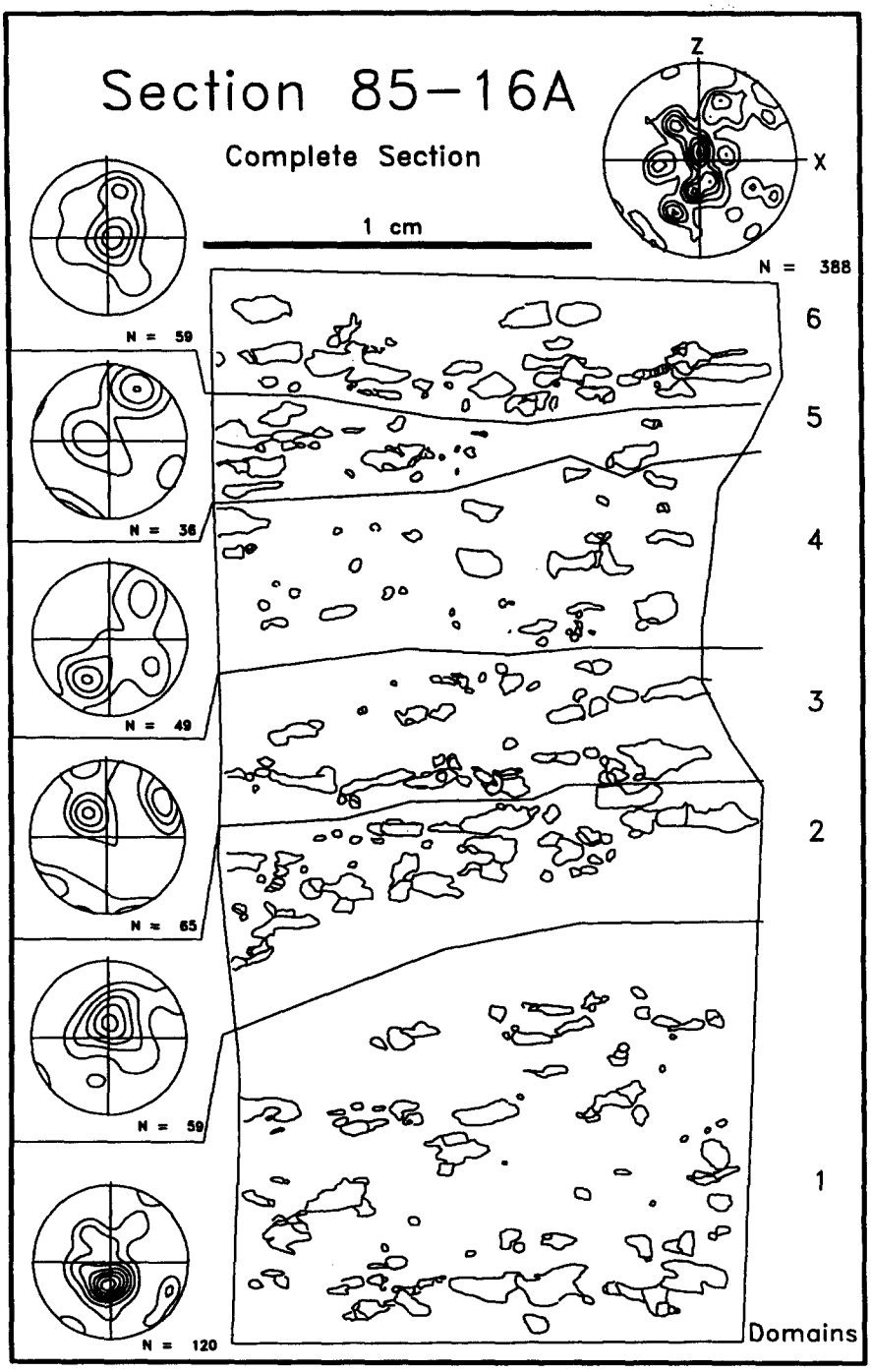

Fig. 8. Domains and domainal fabrics for section 85-16A.

dence of paleostress, as inferred from grain and subgrain size, is compatible with syntectonic grain growth. The presence of preferred crystallographic orientations which can be specifically correlated with individual domains further argues that grain growth and c-axis fabrics result from the same deformational event; it is unlikely that static annealing would cause the strong domainal fabrics shown in Figs. 7–9.

Maxima III are the most prominent maxima when unweighted data are contoured, but weighting of data strengthens a Maximum III and brings out an additional very strong Maximum I. This means that the largest grains have their c-axes preferentially at Maxima I or III positions. Maximum I corresponds to horizontal c-axes, parallel to the foliation but perpendicular to the lineation (Fig. 1). For Maxima III the c-axes are at 45° to the lineation in the *XZ* plane.

Domainal fabrics

Domainal quartz c-axis fabrics have been reported in fine-grained mylonites by Eisbacher (1970), Garcia Celma (1982), Burg (1986), Knipe & Law (1987), Law *et al.* (1990) and others. Compared to those studies, the fabric variations between domains are much more pronounced here; each domain exhibits only one or two

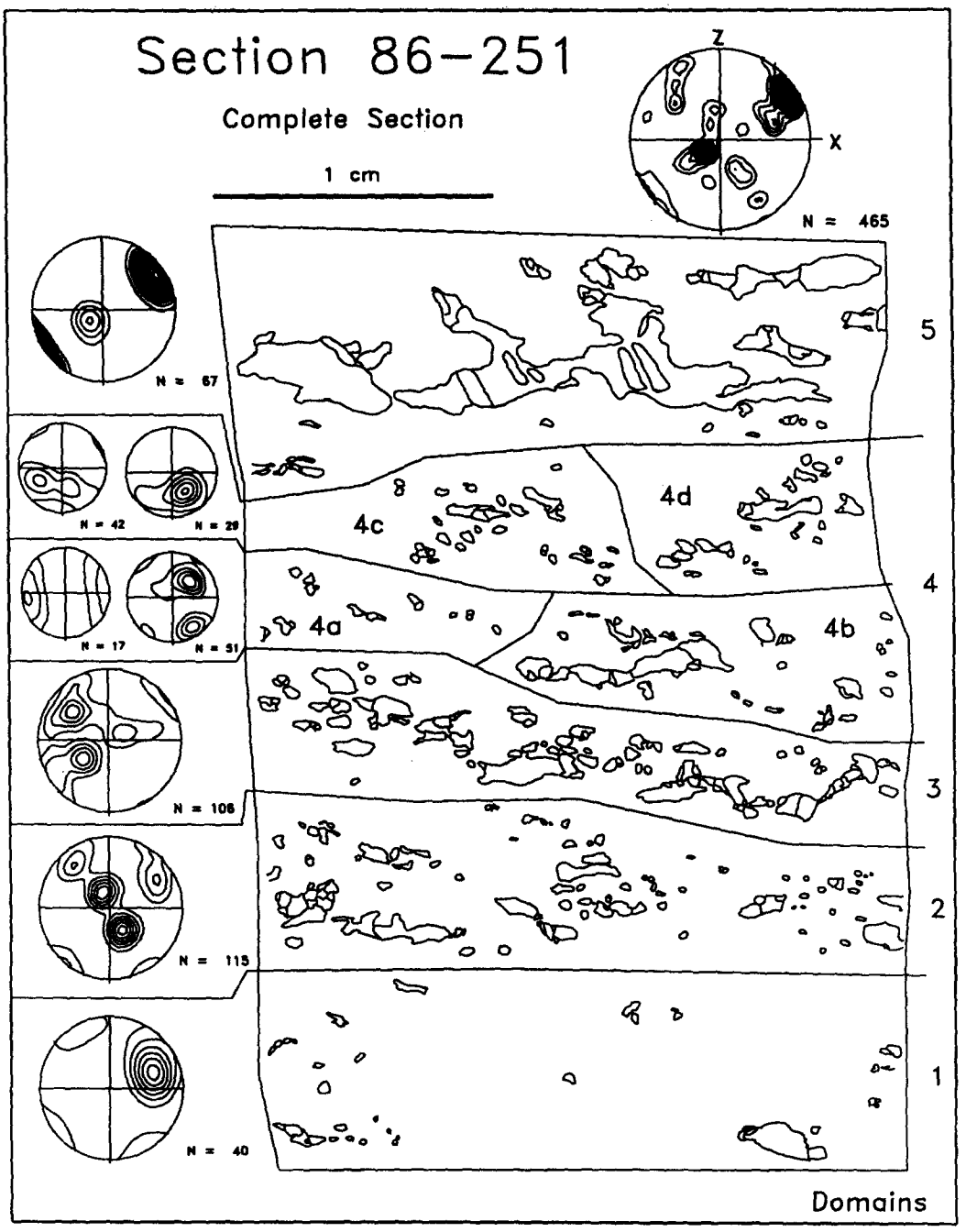

Fig. 9. Domains and domainal fabrics for section 86-251.

of the peaks of the total fabric. In section 85-16 the domainal fabrics alternate from domain to domain, so that two adjacent domains are sufficient to reproduce the complete fabric. In domains in which most quartz grains are adjacent or closely spaced (separated by much less than one grain diameter), the domainal fabric consists primarily of peaks in one of the two Maxima III positions, with or without Maximum I. In contrast, where the quartz grains are widely spaced and evenly distributed throughout the domain (e.g. section 86-251, domain 4) the domainal fabric shows peaks in all four quadrants. In other words, isolated grains may behave independently, whereas the *c*-axes of closely spaced grains cluster around one or two maxima.

Glide systems

We propose that the concentrations of *c*-axes can be explained by assuming that intracrystalline deformation of each individual grain is dominated by a single slip system. The model outlined in a later section proposes a reason why this might be the case.

Maximum III. Basal ⟨*a*⟩ glide has long been considered an important slip system in quartz (e.g. Nicolas & Poirier 1976, Price 1985, Schmid & Casey 1986) and we suggest that it accounts for Maxima III. Grains at Maxima III have their basal plane striking in the same direction as the subvertical foliation but dipping 45°

(Fig. 10). In this position, if basal ⟨a⟩ were active, the resolved shear stress (*RSS*) on that glide system would be maximized for a maximum principal compressive (σ_1) direction perpendicular to both foliation and lineation. This proposed stress direction coincides with the stress orientation inferred by Green *et al.* (1970) from the shape of experimentally deformed quartzite specimens which also yield a quartz *c*-axis crossed girdle fabric. A σ_1 direction bisecting the girdles during coaxial deformation has also been proposed by Hoffman (1972) and by Lister & Dornsiepen (1982). The greater strength of one Maxima III may indicate the existence of an earlier fabric or that the stress–strain history was not strictly coaxial, such as a coaxial overprint on a simple shear Type I fabric (Lister & Williams 1980).

Lister & Dornsiepen (1982) suggest that switch between basal ⟨a⟩ and prism ⟨c⟩ glide may play an important role in the development of these fabrics. Maximum *RSS* for prism ⟨c⟩ glide, in response to the same σ_1 direction, would be obtained when that prism plane and the *c*-direction within it make an angle of 45° with the foliation. The *c*-axis would therefore also be at a Maximum III position. Section 85-16 shows that subgrain boundaries in grains with shallow plunging *c*-axes are parallel to the *c*-axes. The subgrain boundaries can be interpreted as dislocation walls perpendicular to both slip plane and slip direction (Nicolas & Poirier 1976, p. 137); subgrain boundaries thus argue for the operation of basal glide. Subgrain boundaries perpendicular to ⟨c⟩, which might be expected from prism ⟨c⟩ glide, have not been observed here.

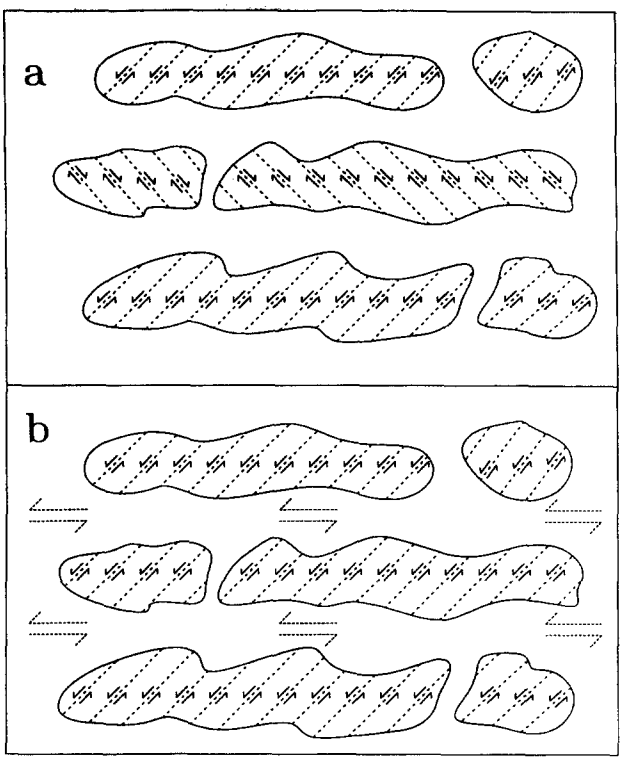

Fig. 10. Schematic representation of the slip directions within individual quartz-rich domains. Foliation horizontal, defined by the layering. (a) Bulk strain approximately progressive pure shear, achieved by slip of both dextral and sinistral domains. (b) A significant component of progressive simple shear may be achieved by the predominance of sinistral domains over dextral ones, and concentration of shear in the relatively weak quartz-poor layers. Stress refraction within the relatively competent quartz-rich domains may maintain the maximum *RSS* direction at approximately 45° to the foliation.

Maximum I. Neither prism ⟨c⟩ nor basal ⟨a⟩ can account for the development of Maximum I in response to the proposed stress. Starkey (1979) and Mancktelow (1987) attribute Maximum I to prism ⟨a⟩ glide. Indeed, use of the prism ⟨a⟩ for shear at 45° to the foliation and lineation would require the *c*-axis to lie at Maximum I. In this position the *RSS* are maximized for the orientation of stresses discussed above.

In summary, we propose that Maximum III and Maximum I result from basal ⟨a⟩ and prism ⟨a⟩ glide, respectively, in response to a stress system in which σ_1 and σ_3 directions are approximately parallel to *Z* and *X*. This implies that the shear direction for the grains preserved for observation was at 45° to the *X* direction. We should note however that *c*-axis measurements alone, in contrast to full lattice orientation data, do not constrain the orientation of either glide system completely. A *c*-axis at Maximum III does constrain a basal glide plane to be perpendicular to that Maximum (Fig. 11), but does not uniquely constrain the glide direction. A *c*-axis at Maximum I only constrains the glide direction to be perpendicular to the *c*-axis, but does not constrain the glide plane. The assumption that each maximum results from the operation of a single glide system within a grain accounts for the fact that the observed fabric consists of maxima rather than girdles.

The model below incorporates grain growth as an important process in the development of the fabric to explain why: (1) a single glide system would operate in each grain; (2) this single glide system should be near its maximum *RSS* orientation in the preserved grains; and (3) the fabric is domainal.

A MODEL FOR DOMAINAL FABRIC DEVELOPMENT

Assumptions

The model relies on the following assumptions:

(1) Quartz grains with *c*-axes at Maxima I or III were deforming through operation of a single glide system. The preference of grains for deforming by a single, favourably oriented glide system even when several systems are available, has been noted by Burg (1986), Urai *et al.* (1986) and Law *et al.* (1990). A likely explanation for this preference for a single slip system is that when more than one glide system operates in a grain, the interaction between glide systems results in strain hardening and in a higher internal strain energy than in grains in which only one glide system operates. This assumption, based on the experimental results of previous workers, is also used by Jessell (1988) in his fabric simulation.

(2) Differences in internal strain energies are suf-

ficient for grains with lower strain energy to consume neighbours with higher strain energy (Poirier 1985). Relatively high strain energy of a grain could be due to the simultaneous operation of two slip systems or the unfavourable orientation of one easy glide system.

(3) The rock is segregated into alternating quartz-rich and quartz-poor layers. This assumption is made to avoid the problem of the origin of the layering, perhaps by some kind of mass transfer. In our model, the origin of layering is independent of that of the *c*-axes fabric, and could either pre-date or be concurrent with the acquisition of that fabric.

No constraint is placed on the initial size of quartz grains, and the current size is set by dynamic recrystallization. Similarly, no constraint is set on the presence of a pre-existing fabric, since it would have been overwritten or at least modified.

Domainal shear

The model focuses on the development of the *c*-axis fabric in quartz-rich lenses such as in section 85-16 and in domain 5 of section 86-251. It is postulated that each domain has developed a unique shear direction oriented approximately at 45° to the foliation, the direction of maximum *RSS* (Fig. 10). The shear direction is approximately in the *XZ* plane, and the sense of shear is either sinistral or dextral. Within domains deforming with a sinistral sense of shear, grains which glide on the basal ⟨*a*⟩ system will have their *c*-axes at Maximum IIIB (Fig. 11). The same domainal shear can also be accomplished by prism ⟨*a*⟩ glide of grains with their *c*-axes at Maximum I. Conversely, within domains deforming with a dextral sense of shear, *c*-axes will plot at Maximum IIIA (Fig. 11, basal glide), as well as at Maximum I (Fig. 11, prism glide). A single shear direction for each individual quartz-rich domain thus accounts for the fact that it shows Maximum I and only one Maximum III (e.g. section 85-16, domains 2–4 and section 86-251, domain 5).

This proposed domainal distribution of shear is similar to the general kinematic model of Cobbold & Gapais (1986) in which simple shear directions within stacked, parallel, planar domains can combine to yield a general bulk strain for the rock. The coherency between adjacent domains imposed by Cobbold & Gapais (1986) is not strictly required for the quartz patches here, particularly when they are separated from each other by wide quartz-poor layers (Fig. 10). It may be significant that the best displayed alternance between dextral and sinistral domains is found for domains 2–4 in section 85-16, in which the quartz-rich lenses are closely spaced.

Variable proportions of sinistral and dextral domains can result in a range of vorticities of the bulk strain away from progressive pure shear (Figs. 10a & b). With an increasing component of progressive simple shear, one might expect rotation of the dominant glide planes into parallelism with the shear foliation. This would result in a dominance of one Maximum III over the other, and the rotation of that maximum toward the perpendicular to the foliation. But stress channeling and refraction within the relatively strong quartz-rich layers may in-

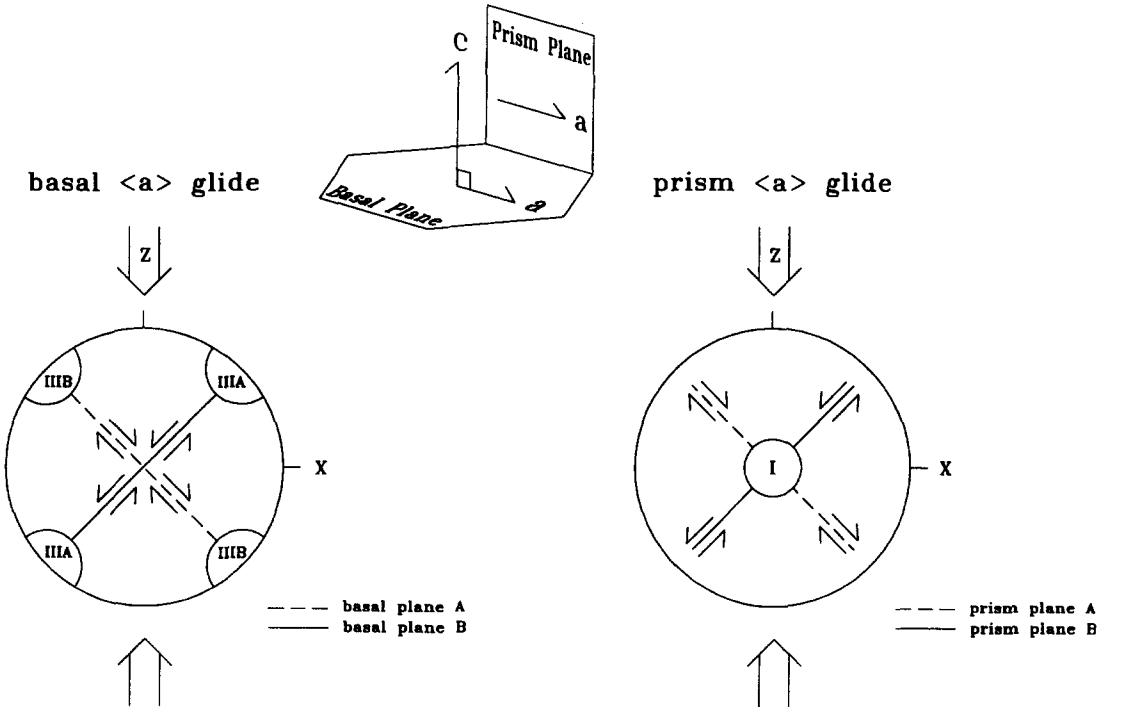

Fig. 11. Schematic description of geometric relations between the basal ⟨*a*⟩ and prism ⟨*a*⟩ glide systems with respect to *c*-axes in quartz. Great circles represent predicted slip planes if glide occurs along maximum *RSS* directions. Point maxima are predicted *c*-axis concentrations for the different glide systems. Dashed great circles would be active in dextral domains, solid great circles in sinistral domains.

stead maintain the maximum *RSS* within them close to 45° to the layering even for significant components of progressive simple shear (Fig. 10b).

Deformation within a single domain

Whereas the bulk strain of the rock can be progressive pure shear, the strain in a single domain is better modelled as progressive simple shear at 45° to the foliation. The combination of grain rotation and recrystallization which we propose is similar to that documented for progressive simple shear experiments in ice by Burg *et al.* (1986). In our model, however, quartz uses two slip systems, prism ⟨*a*⟩ and basal ⟨*a*⟩, instead of just one as in ice. Regardless of which glide system each individual grain uses, grains align their active glide system. As in ice, it is proposed that the successful grains are those which best accommodate the shear strain specific to their domain without strain hardening. These grains are those in which one slip system, parallel to the progressive simple shear direction of the domain, is activated. Their *c*-axes plot near Maximum I (prism ⟨*a*⟩) or one of the Maxima III (basal ⟨*a*⟩).

Bulk rotation of grains and of their glide systems, as outlined by Etchecopar (1977), plays an important role in the progressive deformation of rocks, and indeed in the acquisition of a fabric. Two different processes lead to the rotation of grains. (1) A grain, and its glide system, may be rotated into, or out of, the shear direction for its domain through interaction of neighbouring grains. Physical rotation of grains into an easy-glide position has been proposed by Mancktelow (1987). Conversely, a successful grain and its glide system may also be rotated out of its easy-glide position; this rotation can therefore both create and destroy successful grains. (2) The operation of a glide system itself results in the rotation of that system out of the maximum *RSS* position. Such a grain is therefore no longer 'successful' and will be consumed by a more favourably oriented neighbour.

Within each domain, grain rotation and recrystallization thus continuously provide new successful grains and result in a steady-state orientation of the shear direction, parallel to the maximum *RSS* direction. This continuous renewal of grains can explain why a single shear direction, near the maximum *RSS* orientation, is still preserved in each domain. The limiting end product for the fabric of a quartz-rich domain is that exhibited by section 86-251, domain 5 or section 85-16, domain 6.

Disseminated quartz

In contrast to the domains containing a large patch of quartz, other domains (e.g. section 86-251, domain 4) contain only disseminated quartz grains within a matrix of other minerals that deform by different mechanisms. Such quartz grains are mechanically decoupled from each other and deformation should therefore not result in a strong alternating domainal fabric. Strain imposed on the quartz by these surrounding grains will not lead to the domination of one glide orientation.

CONCLUSIONS

The crucial points of the model can be summarized as follows.

(1) Successful grains deform by a single glide system which is oriented near one maximum *RSS* direction.

(2) Grains within a quartz-rich domain co-operate, using either prism ⟨*a*⟩ or basal ⟨*a*⟩ glide, to allow the whole quartz aggregate to deform by progressive simple shear along the direction of maximum *RSS* (Fig. 10). It should be noted that, in general, this model does not depend on the use of these specific glide systems. It does depend, however, on the build-up of internal strain energy where several glide systems operate simultaneously in a single grain.

(3) Recrystallization and grain rotations result in a steady state orientation of the shear direction for each patch of quartz, parallel to the maximum *RSS* direction, at 45° to the foliation.

(4) The deformation of individual domains, which can be classified as dextral or sinistral, together with 'incoherency' between domains, combine to allow a range of vorticities for the bulk strain of the rock (Figs. 10a & b). The evolution of a domain differs from that in the Cobbold & Gapais (1986) kinematic model in that recrystallization provides a permanent, steady-state resetting of the glide direction parallel to the maximum *RSS* direction, and the coherency constraint is loosened.

In our model, the view of progressive simple shear of a rock differs from the traditional one. Progressive simple shear is generally thought of as a path of deformation which is imposed on a volume of rock by external boundary conditions such as the experimental machine, the rigid parallel walls of a shear zone, etc. In the present model, however, progressive simple shear parallel to the maximum *RSS* direction is the path which is chosen by each quartz-rich aggregate. Both a reason for, and a consequence of, this choice is that the rock is softer where individual domains deform by progressive simple shear, regardless of the boundary conditions imposed on the bulk rock.

Acknowledgements—Support for this work was provided by contracts from the Department of Supplies and Services Canada, and by Natural Sciences and Engineering Research Council operating grants to P.-Y. F. Robin. The manuscript benefited greatly from very constructive comments and suggestions by J.-L. Bouchez, J.-P. Burg, A. R. Cruden, R. D. Law, N. S. Mancktelow, J. Starkey, and an anonymous reviewer.

REFERENCES

Behr, H. J. 1961. Beiträge zur petrographischen und tectonischen Analyse des Sächsischen Granulitgebirges. *Freiberger Forsch.* **C119**, 1–118.

Behr, H. J. 1980. Polyphase shear zones in the granulite belts along the margins of the Bohemian Massif. *J. Struct. Geol.* **2**, 249–254.

Bouchez, J.-L. 1977. Plastic deformation of quartzites at low temperature in an area of natural strain gradient. *Tectonophysics* **39**, 25–50.

Burg, J. P. 1986. Quartz shape fabric variations and *c*-axis fabrics in a ribbon-mylonite: arguments for an oscillating foliation. *J. Struct. Geol.* **8**, 123–131.

Burg, J. P., Wilson, C. J. L. & Mitchell, J. 1986. Dynamic recrystallization and fabric development during the simple shear deformation of ice. *J. Struct. Geol.* **8**, 857–870.

Chayes, F. 1956. *Petrographic Modal Analysis*. John Wiley & Sons, New York.

Christie, J. M. & Ord, A. 1980. Flow stress from microstructures of mylonites: examples and current assessment. *J. geophys. Res.* **85**, 6235–6262.

Cobbold, P. R. & Gapais, D. 1986. Slip-system domains. I. Plane-strain kinematics of arrays of coherent bands with twinned fibre orientations. *Tectonophysics* **131**, 113–132.

Culshaw, N. G. & Fyson, W. K. 1984. Quartz ribbons in high grade granite gneiss: modifications of dynamically formed quartz *c*-axis preferred orientation by oriented grain growth. *J. Struct. Geol.* **6**, 663–668.

Eisbacher, G. H. 1970. Deformation mechanics of mylonitic rocks and fractured granites in Cobequid Mountains, Nova Scotia, Canada. *Bull. geol. Soc. Am.* **81**, 2009–2020.

Etchecopar, A. 1977. A plane kinematic model of progressive deformation in a polycrystalline aggregate. *Tectonophysics* **39**, 121–142.

Fairbairn, H. W. 1949. *Structural Petrology of Deformed Rocks*. Addison Wesley Press, Cambridge, Massachusetts.

Fueten, F. 1989. Deformation of quartzo-feldspathic gneisses in the Thompson Belt, Manitoba. Unpublished Ph.D. Thesis, University of Toronto.

Fueten, F. & Robin, P.-Y. F. 1989. Structural petrology along a transect across the Thompson Belt, Manitoba: dip-slip on the western Churchill–Superior boundary. *Can. J. Earth Sci.* **26**, 1976–1989.

Garcia Celma, A. 1982. Domainal and fabric heterogeneities in the Cap de Creus quartz mylonites. *J. Struct. Geol.* **4**, 443–455.

Green, A. G., Hajnal, Z. & Weber, W. 1985. An evolutionary model of the western Churchill province and western margin of the Superior Province in Canada and the north-central United States. *Tectonophysics* **116**, 281–323.

Green, H. W., Griggs, D. T. & Christie, J. M. 1970. Syntectonic and annealing recrystallization of fine-grained quartz aggregates. In: *Experimental and Natural Rock Deformation* (edited by Paulitsch, P.). Springer, Berlin, 272–335.

Hoffman, J. 1975. Betrachtungen zur Typisierung von Regelsbildern des Quartzteilgefüges (c-Achsenorientierung) von Metamorphiten s. str., Migmatiten und Anatexiten des Saxothuringikums (DDR) unter Berücksichtigung rheologischer Aspekte. *Z. Geol. Wiss.* **3**, 333–361.

Hoffman, J. 1972. Das Quartzteilgefüge von Metamorphiten und Anatexiten, dargestellt am Beispiel des Osterzgebirges (DDR). *Freiberger Forsc.* **C297**, 1–107.

Jessell, M. W. 1988. Simulation of fabric development in recrystallizing aggregates—II. Example model runs. *J. Struct. Geol.* **10**, 779–793.

Knipe, R. D. & Law, R. D. 1987. The influence of crystallographic orientation and grain boundary migration on microstructural and textural evolution in a *S–C* mylonite. *Tectonophysics* **135**, 155–169.

Kohlstedt, D. L. & Weathers, M. S. 1980. Deformation-induced microstructures, paleopiezometers, and differential stresses in deeply eroded fault zones. *J. geophys. Res.* **85**, 6269–6285.

Law, R. D., Schmid, S. M. & Wheeler, J. 1990. Simple shear deformation and quartz crystallographic fabrics: a possible natural example from the Torridon area of NW Scotland. *J. Struct. Geol.* **12**, 29–45.

Lister, G. S. & Dornsiepen, U. F. 1982. Fabric transitions in the Saxony granulite terrain. *J. Struct. Geol.* **4**, 81–92.

Lister, G. S., Paterson, M. S. & Hobbs, B. E. 1978. The simulation of fabric development in plastic deformation and its application to quartzite: the model. *Tectonophysics* **45**, 107–158.

Lister, G. S. & Williams, P. F. 1980. Fabric development in shear zones: theoretical controls and observed phenomena. *J. Struct. Geol.* **1**, 283–297.

Mancktelow, N. S. 1987. Atypical textures in quartz veins from the Simplon Fault zone. *J. Struct. Geol.* **9**, 995–1006.

McQueen, H. J. & Jonas, J. J. 1975. Recovery and recrystallization during high temperature deformation. In: *Treatise on Materials Science and Technology* (edited by Arsenault, R. J.), Vol. 6, 393–493.

Means, W. D. & Dong, H. G. 1982. Some unexpected effects of recrystallization on the microstructures of materials deformed at high temperature. *Mitt. geol. Inst. ETH, Neue Folge* **239a**, 205–207.

Mercier, J.-C. C., Anderson, D. A. & Carter, N. L. 1977. Stress in the lithosphere: inferences from steady state flow in rocks. *Pure & Appl. Geophys.* **115**, 199–226.

Nicolas, A. & Poirier, J. P. 1976. *Crystalline Plasticity and Solid-state Flow in Metamorphic Rocks*. John Wiley & Sons, London.

Ord, A. & Christie, J. M. 1984. Flow stresses from microstructures in mylonitic quartzites of the Moine Thrust zone, Assynt area, Scotland. *J. Struct. Geol.* **5**, 639–654.

Paktunç, A. D. & Baer, A. J. 1986. Geothermobarometry of the northwestern margin of the Superior Province: Implications for its tectonic evolution. *J. Geol.* **94**, 381–394.

Poirier, J.-P. 1985. *Creep of Crystals*. Cambridge Earth Science Series, Cambridge University Press, Cambridge.

Price, G. P. 1985. Preferred orientations in quartzites. In: *Preferred Orientation in Deformed Metals and Rocks: An Introduction to Modern Texture Analysis* (edited by Wenk, H.-R.). Academic Press, Orlando, 385–406.

Robin, P.-Y. F. & Jowett, C. E. 1986. Computerized density contouring and statistical evaluation of orientation data using counting circles and continuous weighting functions. *Tectonophysics* **121**, 207–223.

Sander, B. 1970. *An Introduction to the Study of Fabrics of Geological Bodies*. Pergamon Press, Oxford.

Schmid, S. M. & Casey, M. 1986. Complete fabric analysis of some commonly observed quartz *c*-axis patterns. *Am. Geophys. Un. Geophys. Monogr.* **36**, 263–286.

Scoates, R. F. J., Macek, J. & Russell, J. K. 1977. Thompson Nickel Belt Project. Manitoba Mineral Resources Division, Geological Survey, Report on Field Activities 1977, 47–53.

Starkey, J. 1979. Petrofabric analysis of Saxony Granulites by optical and X-ray diffraction methods. *Tectonophysics* **58**, 201–219.

Turner, F. J. & Weiss, L. E. 1963. *Structural Analysis of Metamorphic Tectonites*. McGraw-Hill, New York.

Twiss, R. J. 1977. Theory and applicability of recrystallized grain size paleopiezometer. *Pure & Appl. Geophys.* **115**, 227–244.

Twiss, R. J. 1986. Variable sensitivity piezometric equations for dislocation density and subgrain diameter and their relevance to olivine and quartz. *Am. Geophys. Un. Geophys. Monogr.* **36**, 247–261.

Urai, J. L. & Humphreys, F. J. 1981. The development of shear zones in polycrystalline camphor. *Tectonophysics* **78**, 677–685.

Urai, J. L., Means, W. D. & Lister, G. S. 1986. Dynamic recrystallization of minerals. *Am. Geophys. Un. Geophys. Monogr.* **36**, 161–199.

Weathers, S. M., Bird, J. M., Cooper, R. F. & Kohlstedt, D. L. 1979. Differential stress determined from the deformation-induced microstructures of the Moine Thrust zone. *J. geophys. Res.* **84**, 7495–7509.

Weber, W. & Scoates, R. F. J. 1978. Archean and Proterozoic metamorphism in the northwestern Superior Province and along the Churchill–Superior boundary, Manitoba. *Geol. Surv. Pap. Can.* **78-10**, 5–16.